Axi-symmetric analysis of vertically inhomogeneous elastic multilayered systems

J. W. Maina
CSIR Built Environment, Pretoria, South Africa

Y. Ozawa & K. Matsui
Tokyo Denki University, Saitama, Japan

ABSTRACT: The importance of accounting for material nonlinearity and anisotropic behavior in order to improve the resilient models for pavement materials and numerical analysis is presented in this paper. Effects of material inhomogeneity on the pavement primary resilient responses are investigated by way of worked examples of hypothetical three-layer system, which was analyzed by considering homogenous and inhomogeneous material properties in each of the three layers. Effect of a inhomogeneity parameter that is used in the z-dependent exponential model on the resilient responses in the pavement structure was also investigated. This paper reports on the formulation as well as the findings from detailed analyses that were conducted.

1 INTRODUCTION

1.1 *General*

Methods for structural design of pavements have been shifting from empirical to mechanistic-empirical based approach. Several software based on multilayer linear elastic (MLLE) theory have already been developed for this purpose. For example, the AASHTO Pavement design guide for flexible pavements is shifting from an experience (or purely empirical) based design method to a mechanistic-empirical (M-E) design method. The latter approach requires an elastic MLLE analysis engine to compute responses of interest and use empirically established models to determine airport and road pavement distresses like fatigue cracking of asphalt concrete layer or rutting (plastic deformation) of the pavement system. In Europe, a study was commissioned to evaluate a number of widely used software for MLLE analysis and a report was released on the Advanced Models for Analytical Design of European Pavement Structures (AMADEUS, 2000). In Japan, Japan Society of Civil Engineers (JSCE) published a third library - an introduction to pavement structural analysis. All these indicate that MLLE method play an important part in pavement design and analysis.

1.2 *Material inhomogeneity*

Majority of the standard methods for MLLE analysis and evaluation of road and airport pavements were developed based on the assumption that each layer within the pavement structure is linear elastic, homogeneous and isotropic. However, in the recent past, several researchers have shown the importance of accounting for non-linearity and anisotropic material properties in order to improve the resilient models for pavement materials and numerical analysis (Gazetas, 1982, Graham and Houslby, 1983, and Correia, 1999). These behaviors can be attributed to pavement material physical properties and the way they are constructed by way of compaction, which results in variable elastic modulus with depth. Moreover, for the case of asphalt concrete layer, its behavior is also temperature sensitive and varies with depth as well. All the these facts call for numerical analysis methods to be developed in such a way as to take into consideration the variation of elastic modulus of pavement layer materials with depth.

Tanigawa et al (1997) assumed the following function to express the depth dependent of elastic shear modulus for a semi-infinite layer:

$$G(z) = G_0 \left(\frac{z}{a} + 1 \right)^m, m \geq 0 \tag{1}$$

Wang *et al* (2003, 2006) presented extensive summary of numerous existing analytical/numerical solutions for inhomogeneous isotropic media due to a circular load. They presented solutions for the displacements and stresses along the axi-symmetric axis due to uniformly distributed circular load. Their findings indicated that vertical displacement and vertical normal stress are greatly influenced by the material inhomogeneity and degree of anisotropy.

In this study, authors applied Hankel transform directly to the governing equations of a multilayered system and derived solutions for the case where the system comprises of an inhomogeneous layer. Further, the influence of material inhomogeneity on the resilient responses (surface displacement, normal and horizontal strains) was evaluated.

2 THEORETICAL DEVELOPMENT

2.1 *Z-dependent model*

In this research, elastic modulus of a material is assumed to be constant in the horizontal direction but inhomogeneous in the vertical direction, where it varies exponentially with depth. Materials that behave in this manner have been named z-dependent materials while layers containing these kinds of materials are called z-dependent layers. By ignoring body forces, equilibrium equations in cylindrical coordinate system are formulated as follows:

$$\frac{\partial \sigma_r}{\partial r} + \frac{\partial \tau_{rz}}{\partial z} + \frac{\sigma_r - \sigma_\theta}{r} = 0 \tag{2a}$$

$$\frac{\partial \tau_{rz}}{\partial r} + \frac{\partial \sigma_z}{\partial z} + \frac{\tau_{rz}}{r} = 0 \tag{2b}$$

where σ_r is normal stress in the r-axis direction, τ_{rz} is shear stress along $r-z$-plane, σ_θ is normal stress in the circumferential (θ) direction and finally, σ_z is normal stress in the z-axis direction. Displacement in the r-axis direction can be represented as $u = u(r, z)$ and displacement in the z-axis direction can be represented as $w = w(r, z)$. For axi-symmetric case, displacement in the circumferential direction is zero, while strains related to the listed stresses are represented as ε_r, ε_θ, ε_z, and γ_{rz}. Similar to the homogeneous case, strain-displacement relationship is as follows:

$$\varepsilon_r = \frac{\partial u}{\partial r}, \ \varepsilon_\theta = \frac{u}{r}, \ \varepsilon_z = \frac{\partial w}{\partial z}, \ \gamma_{rz} = \frac{\partial u}{\partial z} + \frac{\partial w}{\partial r} \tag{3}$$

The difference between homogeneous and inhomogeneous materials is on the formulation of stress-strain relationship, whereby in this study, variation of elastic modulus with depth is represented in an exponential form as follows:

$$E(z) = E_0 \, e^{-bz} \tag{4}$$

where b is the inhomogeneity parameter. Strain-stress relationship can be written in a matrix form as:

$$\begin{Bmatrix} \varepsilon_r \\ \varepsilon_\theta \\ \varepsilon_z \\ \gamma_{rz} \end{Bmatrix} = \begin{bmatrix} 1/E(z) & -\nu/E(z) & -\nu/E(z) & 0 \\ -\nu/E(z) & 1/E(z) & -\nu/E(z) & 0 \\ -\nu/E(z) & -\nu/E(z) & 1/E(z) & 0 \\ 0 & 0 & 0 & 1/\mu(z) \end{bmatrix} \begin{Bmatrix} \sigma_r \\ \sigma_\theta \\ \sigma_z \\ \tau_{rz} \end{Bmatrix} \tag{5}$$

Utilizing Lame's constants $\lambda(z)$ and $\mu(z)$, where:

$$\lambda(z) = \frac{\nu E(z)}{(1+\nu)(1-2\nu)} \quad , \quad \mu(z) = \frac{E(z)}{2(1+\nu)}$$

Stress-strain relationship is represented as:

$$\begin{Bmatrix} \sigma_r \\ \sigma_\theta \\ \sigma_z \\ \tau_{rz} \end{Bmatrix} = \begin{bmatrix} \lambda+2\mu & \lambda & \lambda & 0 \\ \lambda & \lambda+2\mu & \lambda & 0 \\ \lambda & \lambda & \lambda+2\mu & 0 \\ 0 & 0 & 0 & \mu \end{bmatrix} \begin{Bmatrix} \varepsilon_r \\ \varepsilon_\theta \\ \varepsilon_z \\ \gamma_{rz} \end{Bmatrix} \tag{6}$$

Substituting equation (3) into equation (6) and rearrange, yields:

$$\sigma_r = (\lambda+\mu)\frac{\partial u}{\partial r} + \lambda\frac{u}{r} + \lambda\frac{\partial w}{\partial z} \tag{7a}$$

$$\sigma_\theta = \lambda\frac{\partial u}{\partial r} + (\lambda+\mu)\frac{u}{r} + \lambda\frac{\partial w}{\partial z} \tag{7b}$$

$$\sigma_z = \lambda\frac{\partial u}{\partial r} + \lambda\frac{u}{r} + (\lambda+\mu)\frac{\partial w}{\partial z} \tag{7c}$$

$$\tau_{rz} = \mu\left(\frac{\partial u}{\partial z} + \frac{\partial w}{\partial r}\right) \tag{7d}$$

Further substitution of equation (7) into equation (2) and rearrange, gives:

$$(\lambda+2\mu)\left(\frac{\partial^2}{\partial r^2} + \frac{\partial}{\partial r}\left(\frac{1}{r}\frac{\partial}{\partial r}\right) + \frac{\mu}{\lambda+2\mu}\left(-b+\frac{\partial}{\partial z}\right)\frac{\partial u}{\partial z}\right) - \frac{\partial}{\partial r}\left(b\mu - (\lambda+\mu)\frac{\partial}{\partial z}\right)w = 0 \tag{8a}$$

$$\left((\lambda+\mu)\frac{\partial}{\partial z} - b\lambda\right)\left(\frac{\partial}{\partial r} + \frac{1}{r}\right)u + \mu\left(\frac{\partial^2}{\partial r^2} + \frac{1}{r}\frac{\partial}{\partial r} - b\frac{\lambda+2\mu}{\mu}\frac{\partial}{\partial z} + \frac{\lambda+2\mu}{\mu}\frac{\partial^2}{\partial z^2}\right)w = 0 \tag{8b}$$

Boundary conditions considering a uniformly distributed surface $(z=0)$ load, p over an area of radius, a are such that;

$$\begin{aligned} & z=0. \quad r \le a \quad \sigma_z = -p \\ & r > a \quad \sigma_z = 0 \\ & r \ge 0 \quad \tau_{rz} = 0 \end{aligned} \tag{9}$$

Resilient response solutions may be obtained through Hankel transform and then Hankel inverse transforms. The general procedure is thorough explained in Maina and Matsui (2004).

3 VALIDATION AND ACCURACY OF Z-DEPENDENT ALGORITHM

An algorithm for z-dependent multilayered structure was developed based on the approach explained in the previous section. And in order to validate and confirm accuracy of this algorithm, its results were compared with results from GAMES software, which deals with homogeneous materials. Since GAMES software cannot perform analysis for z-dependent materials, the z-dependent layer of interest (in this case, first layer) was subdivided into several layers of homogeneous material. An approximate analysis was, thereafter, performed using GAMES and results were compared with those from a z-dependent algorithm.

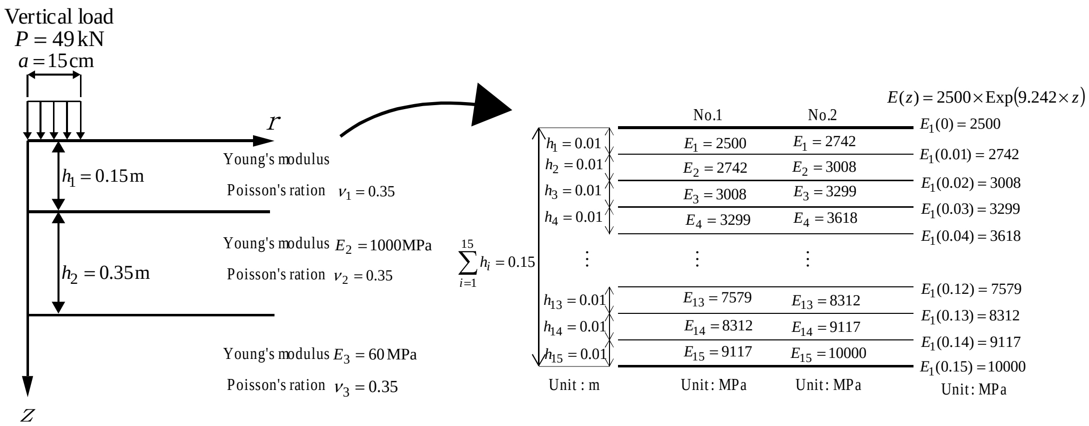

Figure 1. Hypothetical pavement model.

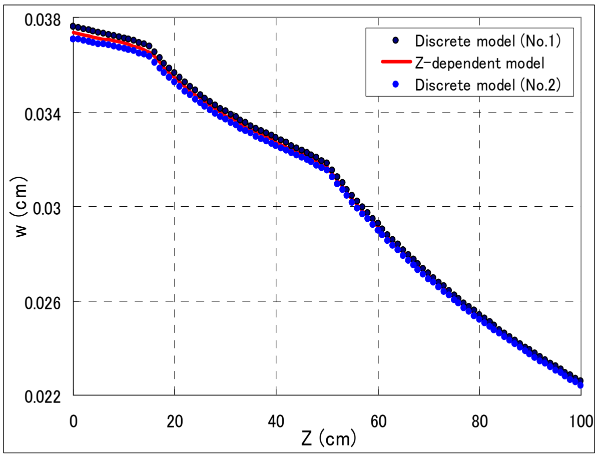

Figure 2. Analytical results for the three models.

The hypothetical pavement model used is shown in Figure 1. Only the first layer is assumed to be z-dependent layer. In equation (3), b and E_0 were determined such that elastic modulus of the upper part ($z = 0m$) of the first layer would be 2500MPa and the bottom part would to be 1000MPa. The right hand side of Figure 1 shows the elastic moduli for two discrete models together with the values determined from equation (3).

The procedure to generate the discrete layers for the two models shown in Figure 1 was as follows:

- The first pavement layer, which was 0.15m thick, was subdivided into 15 layers, 0.01m thick each.
- For model 1, each layer was assigned an elastic modulus value, which was similar to the value determined at its top position using equation (3).
- For model 2, each layer was assigned an elastic modulus value, which was similar to the value determined at its bottom position using equation (3).

The analytical results are shown in Figure 2. This figure shows displacement with depth below the centre of the load (r = 0). Displacements determined from z-dependent model were in between the displacements determined using the two discrete models. There was a good agreement between displacements determined from the z-dependent algorithm and displacements from discrete models which validates the theory developed and confirmation of the accuracy of z-dependent algorithm.

4 ANALYSIS FOR Z-DEPENDENT MATERIALS

4.1 *Development of analytical model*

In order to evaluate how variation of elastic modulus with depth within a particular pavement layer can affect resilient responses when compared to responses for homogenous materials, a three layer pavement model was selected. For each analytical case considered, material in only one layer was assumed to be z-dependent. Analyses for surface displacement, normal and horizontal strains were performed and compared to the case where all the layers were assumed to be homogeneous. Table 1 shows parameters E_0 and b for different types of z-dependent models that were considered, while Figure 3 shows the isotropic and homogenous pavement model that was used for benchmarking and called Type0. External uniformly distributed load was 49kN, which was assumed to act over an area of radius 0.15m.

Table 1..Parameters for various z-dependent models

		Unit	layer1				layer 2		layer 3					
			Type1	Type2	Type3	Type4	Type5	Type6	Type7	Type8	Type9	Type10	Type11	Type12
Parameter	b	1/m	-9.24	-5.00	5.00	9.24	-0.10	-0.50	-0.10	-0.50	-1.00	-2.00	-5.00	-10.00
	E_0	MPa	2500.0	3436.4	7275.0	10000.0	500.0	2000.0	60.0	60.0	60.0	60.0	60.0	60.0

4.2 *Z-dependent model (first layer only)*

Figure 4 shows pavement model that was used for analysis considering z-dependent material in the first layer. Elastic modulus of the first layer is assumed to be a function of z, whereby E_0 is the elastic modulus at the top position of the first layer and a positive parameter b represents a softening layer, while a negative parameter b represents a stiffening layer. By varying the values of E_0 and b, four different models were developed, namely (Type1 ~ Type4) and analyses using values from each of the four models were performed. Layer moduli values for the different models are graphically presented in Figure 5. E_0 and b values were selected such that, for each model, the median value of elastic modulus in the first layer would be 5000MPa.

Figure 6(a) shows results of surface displacements for models Type0, Type1, and Type4. Below the load centre, deflections from a model depicting a softening top layer (Type4) were smaller compared to those from a stiffening layer (Type1). For the three models considered, the difference in displacements was evident in the vicinity of the loaded region and insignificant at points beyond 3 times the load radius.

Figure 6(b) shows variation of normal vertical strain (ε_z) at points along the $z-$axis and below the load centre ($r=0$). These are analytical results for all the 5 models (Type0 ~ Type4). For each model, a discontinuity of strain is observed at layer interfaces. In the first layer where z-dependent material was assumed, differences are observed in strain (ε_z) trends among the five models. Type0 shows tensile strain on pavement surface although a compressive stress $\sigma_z = -0.707\text{MPa}$ is acting. The reason for this phenomenon could be attributed to relatively higher horizontal compressive stresses $\sigma_x = \sigma_y = -1.280\text{MPa}$ when combined with Poisson's ratio may result in tensile strain in the z-direction. Compared with model Type0, layer softening models (Type3 and Type4) had higher tensile strains on the surface and higher compressive strain at the bottom of the first layer. Layer stiffening models had relatively lower results. Type1 layer stiffening model resulted in compressive normal strain (ε_z) on the surface. All the five models (Type0 ~ Type4) were set in such a way that the median elastic modulus would be the same. However, strain results were similar at about 0.05m from the surface. Material inhomogeneity in the first layer had higher influence on normal vertical strain results in the third layer than in the second layer.

Figure 6(c) shows variation of normal horizontal strain (ε_r) at points along the $z-$axis and below the load centre ($r = 0$). Again, these are analytical results for all the 5 models (Type0 ~ Type4) and they all show very comparable compressive strains at the surface. At the bottom of the layer the results show tensile strains whose trends are opposite to the layer moduli. Type4 had the highest value and Type1, the smallest. The influence of material inhomogeneity in the first layer on horizontal normal strain results in the third layer was insignificant.

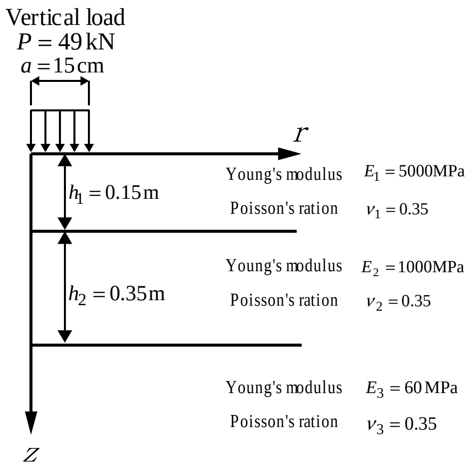

Figure 3. Homogeneous pavement model.

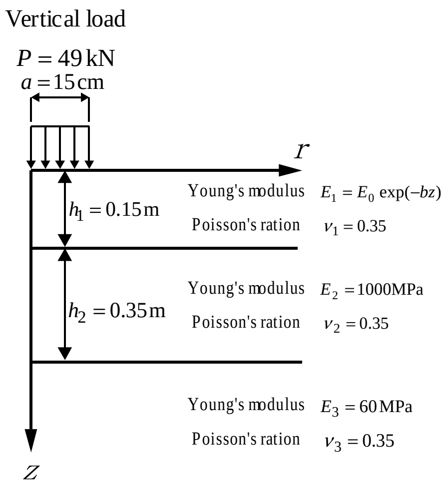

Figure 4. Inhomogeneous (first layer) model.

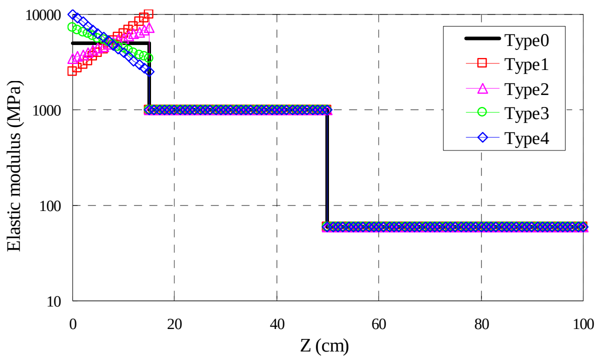

Figure 5. Distribution of layer moduli with depth.

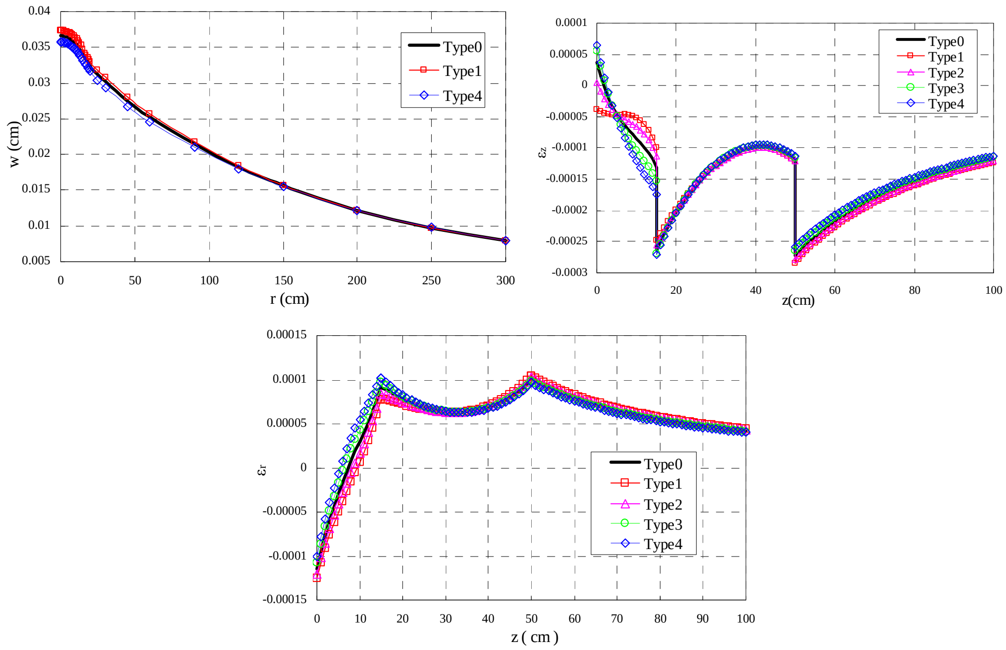

Figure 6. Results for displacements and strains considering inhomogeneous first layer.

4.3 *Z-dependent model (second layer only)*

Figure 7 shows pavement model that was used for analysis considering z-dependent material in the second layer. Values of E_0 and b were varied to form two models (Type5 and Type6) and analyses were performed. E_0 and b values were selected such that, for each model, the median value of elastic modulus in the second layer would be 1000MPa.

Figure 9(a) shows surface displacements using the two models. The effect of material inhomogeneity is evident between the load edge to 10 times the load radius (i.e. r =15cm ~ 150 cm). Compared to Type0, surface displacement results from layer stiffening model (Type5) were smaller and those from layer softening model (Type6) were bigger.

Figure 9(b) shows variation of normal vertical strain (ε_z) at points along the $z-$axis and below the load centre ($r=0$). Similar to the previous case of material inhomogeneity in the first layer, a discontinuity of normal vertical strain (ε_z) is observed at layer interfaces. Further, the effect of material inhomogeneity on the normal vertical strain within the second layer is considerable.

Figure 9(c) shows variation of normal horizontal strain (ε_r) at points along the $z-$axis and below the load centre ($r=0$). There is continuity of normal horizontal strain at layer interfaces. Because of this continuity at layer interfaces, the effect of material inhomogeneity on the normal horizontal strain (ε_r) in the lower part of the first layer, within the second layer and upper part of the bottom layer is considerable.

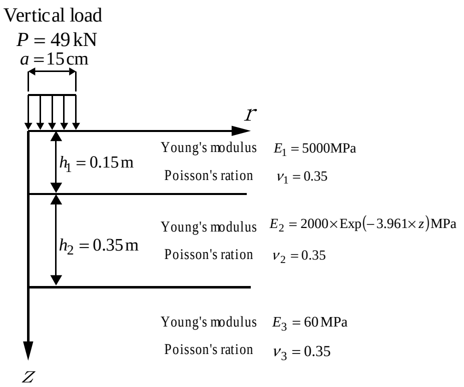

Figure 7. Inhomogeneous (second layer) model

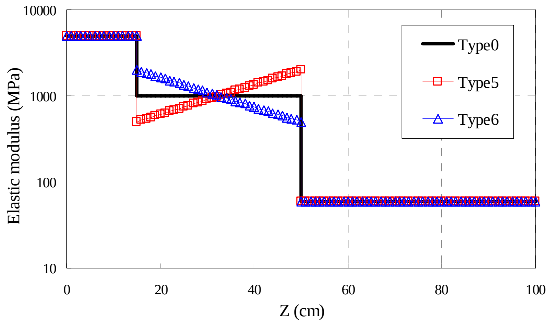

Figure 8. Distribution of layer moduli with depth.

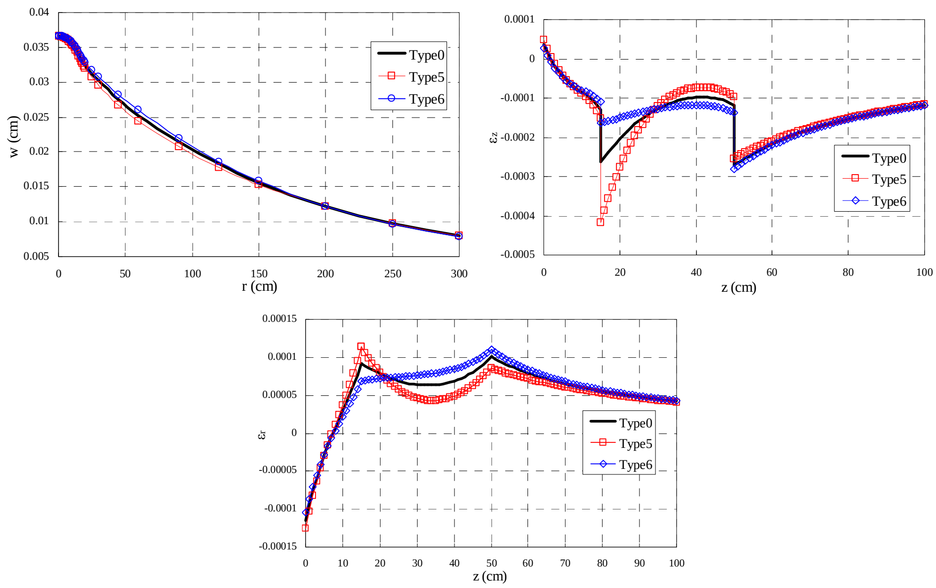

Figure 9. Results for displacements and strains considering inhomogeneous second layer.

4.4 *Z-dependent model (third layer only)*

Figure 10 shows pavement model that was used for analysis considering z-dependent material in the third layer. E_0 was held constant and parameter b was varied to form six models (Type7 ~ Type12) and analyses were performed. As $z \to \infty$, layer softening model for semi-infinite subgrade layer would result in zero elastic modulus and infinity displacement, hence only layer stiffening models were used. Elastic moduli for different z-dependent models are graphically presented in Figure 11.

Figure 12(a) shows surface displacements for four of the models used. As parameter b increases, surface displacements decrease, which is an indication that material inhomogeneity in the subgrade layer significantly affect pavement surface displacements.

Figure 12(b) shows variation of normal vertical strain (ε_z) at points along the $z-$axis and below the load centre ($r=0$). The effect of material inhomogeneity in the subgrade layer on normal vertical strain in the first and second layer was found to be insignificant. However, ε_z in the third layer was highly influenced by material property within the layer. Figure 12(c) shows variation of normal horizontal strain (ε_r) at points along the $z-$axis and below the load centre ($r=0$). Due to continuity of the normal horizontal strain at layer interfaces, the effect of material inhomogeneity in the third layer on the normal horizontal strain (ε_r) is significant within the lower part of the second layer and the whole of the third layer.

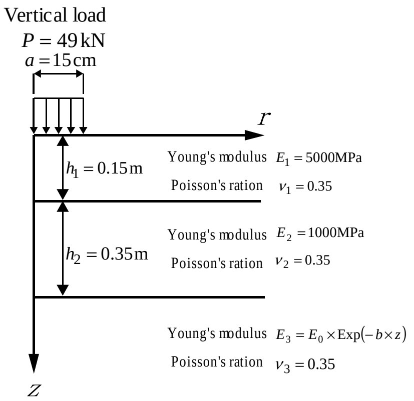

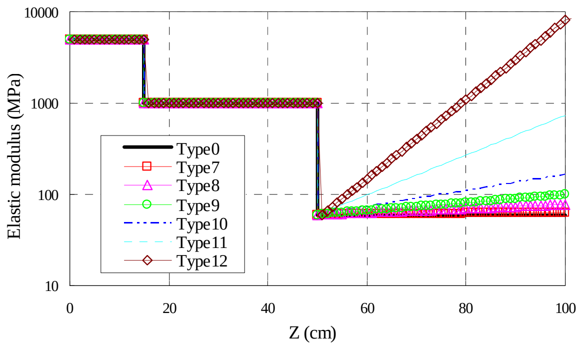

Figure 10. Inhomogeneous (third layer) model. Figure 11. Distribution of layer moduli with depth.

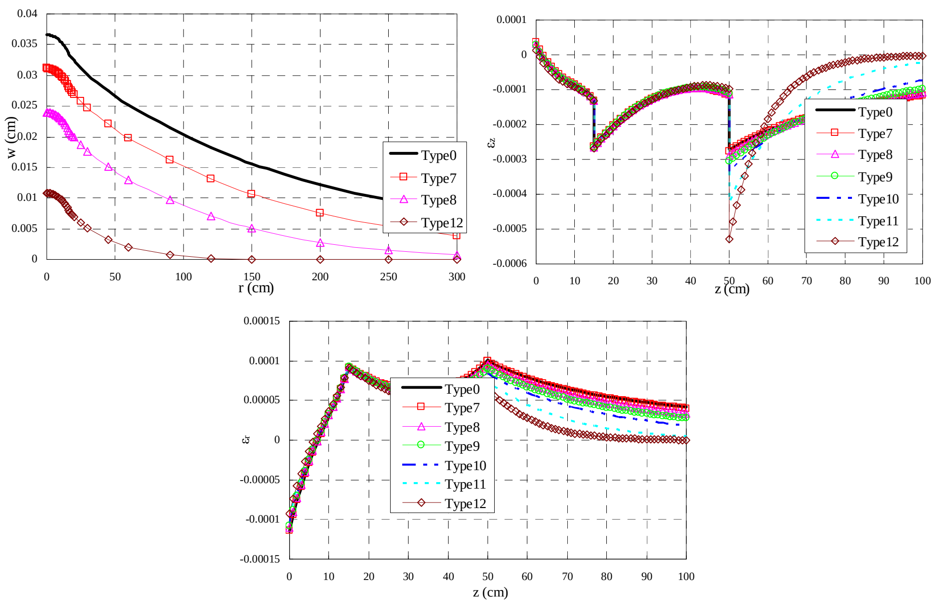

Figure 12. Results for displacements and strains considering inhomogeneous third layer.

5 OBSERVATION AND CONCLUDING REMARKS

Algorithm for multilayered linear elastic analysis considering z-dependent materials has been developed based on the approach presented in this paper.

1. Analytical results for z-dependent algorithm agreed well with GAMES results when layer discretization was performed. This confirms accuracy of the algorithm developed.
2. When the top pavement layer is considered to be z-dependent, surface displacements for layer stiffening models were bigger than for layer softening models. The effect of z-dependent top layer was smaller for layer stiffening models than for layer softening models.
3. The effect of z-dependent second layer on the surface displacement was negligible.
4. There were significant effects of the magnitude of parameter b for z-dependent subgrade on surface displacements

5. Because of discontinuity at layer interfaces, normal vertical strain (ε_z) was only affected in the layer that was considered to be z-dependent.
6. Because of continuity at layer interfaces, normal horizontal strain (ε_r) in the layer that was considered to be z-dependent as well as in parts of adjacent layers close to the interface with z-dependent layer was affected.

6 REFERENCES

The Committee on Pavement Engineering, JSCE. 2005. *Introduction to Pavement Structural Analysis Based on Multi-layered Elastic Systems –Application with GAMES (General Analysis of Multi-layered Elastic Systems)* -. Pavement Library 3. Maruzen. Tokyo, Japan.

Gazetas, G. 1982. Stresses and Displacements in Cross-Anisotropic Soils. *Journal of Geotechnical Engineering, ASCE*, Vol. 108, No. GT4. pp.532-554.

Graham, J. and Houlsby G.T. 1983. Anisotropic Elasticity of Natural Clay, *Geotechnique*, Vol.33, No. 2, pp.164-181.

Correia, A.G.(ed). 1999. Unbound Granular Materials, Laboratory Testing, in-situ testing and modelling, *Proceedings of an International Workshop on Modelling and Advanced Testing for Unbound Granular Materials*. Lisbon.

Maina, J. W. and K . Matsui. Developing Software for Elastic Analysis of Pavement Structure Responses to Vertical and Horizontal Surface Loadings. Transportation Research Records, No. 1896, pp. 107-118., 2004.

Tanigawa, Y., Jeon, S., and Hata, T. 1997. Analytical Development of Axisymmetrical Elastic Problem for Semi-Infinite Body with Kassir's Nonhomogeneous Material Property. Japan Society of Mechanical Engineers. Vol. 63. No. 608. pp.86-93.

Wang, D.C., Tzeng, C.S. Pan, E. and Liao, J.J. 2003. Displacements and Stresses due to a vertical point in a inhomogeneous transversely isotropic half space. *International Journal of Rock Mechanics and Mining Sciences*, 40(5), 667-685.

Wang, D.C., Pan, E. Tzeng, C.S., Feng H. and Liao, J.J. 2006. Displacements and Stresses due to a uniform vertical circular load in an inhomogeneous cross-anisotropic half space. *International Journal of Geomechanics* , Vol. 6, No.1, 1-10.